CHAPTER 4

RESULTS AND DISCUSSION

4.1 Performance of SILEPE Model

The performance of the SILEPE model in southwest monsoon forecasts is tested by comparison between observed wind speed and direction pattern of NCEP and the forecast at the same time. The results in Figure 4.1 show that patterns of Case A and Case B which have the same pattern with NCEP reanalysis data in the black box. The experiment cases for testing the performance of the model are shown in Table 3.3

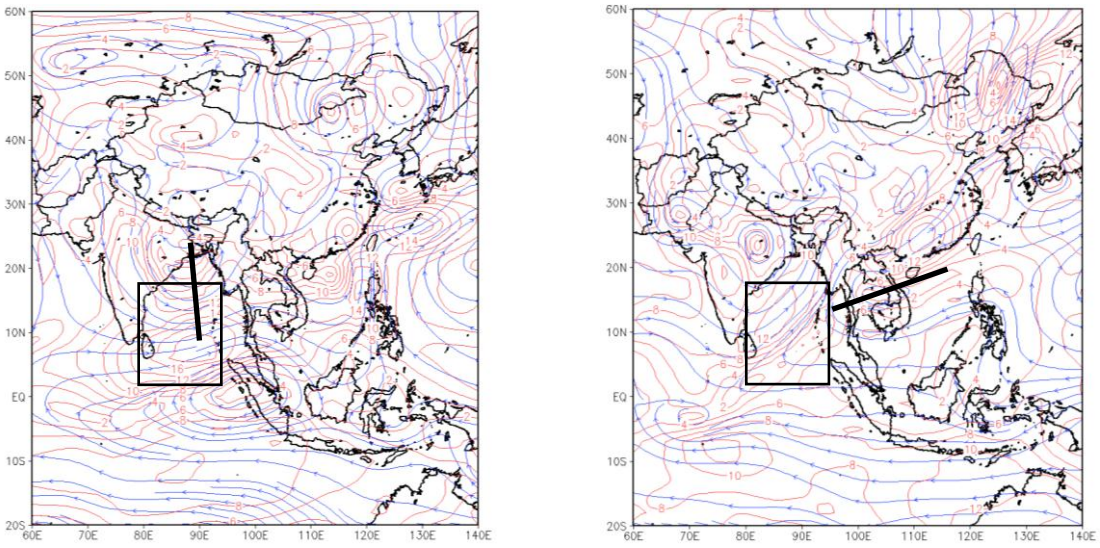

(a) Initial data from NCEP for Case A (b) Initial data from NCEP for Case B

Figure 4.1 Comparison between NCEP 850 hPa wind initial data of (a) active summer monsoon for Case A and (b) summer monsoon break for Case B. The black box is the study domain.

The results in Figure 4.1 show wind direction patterns from NCEP for (a) active summer monsoon for Case A and (b) summer monsoon break for Case B. Figure 4.1(a) shows a trough over the Bay of Bengal when monsoon westerlies are enhanced along a latitudinal band within 5°N–10°N as indicated by the dark-black line. In Figure 4.1(b), the trough is formed over Indochina.

The results from the SILEPE model for Case A are compared with NCEP reanalysis data at the same time in Figure 4.2.

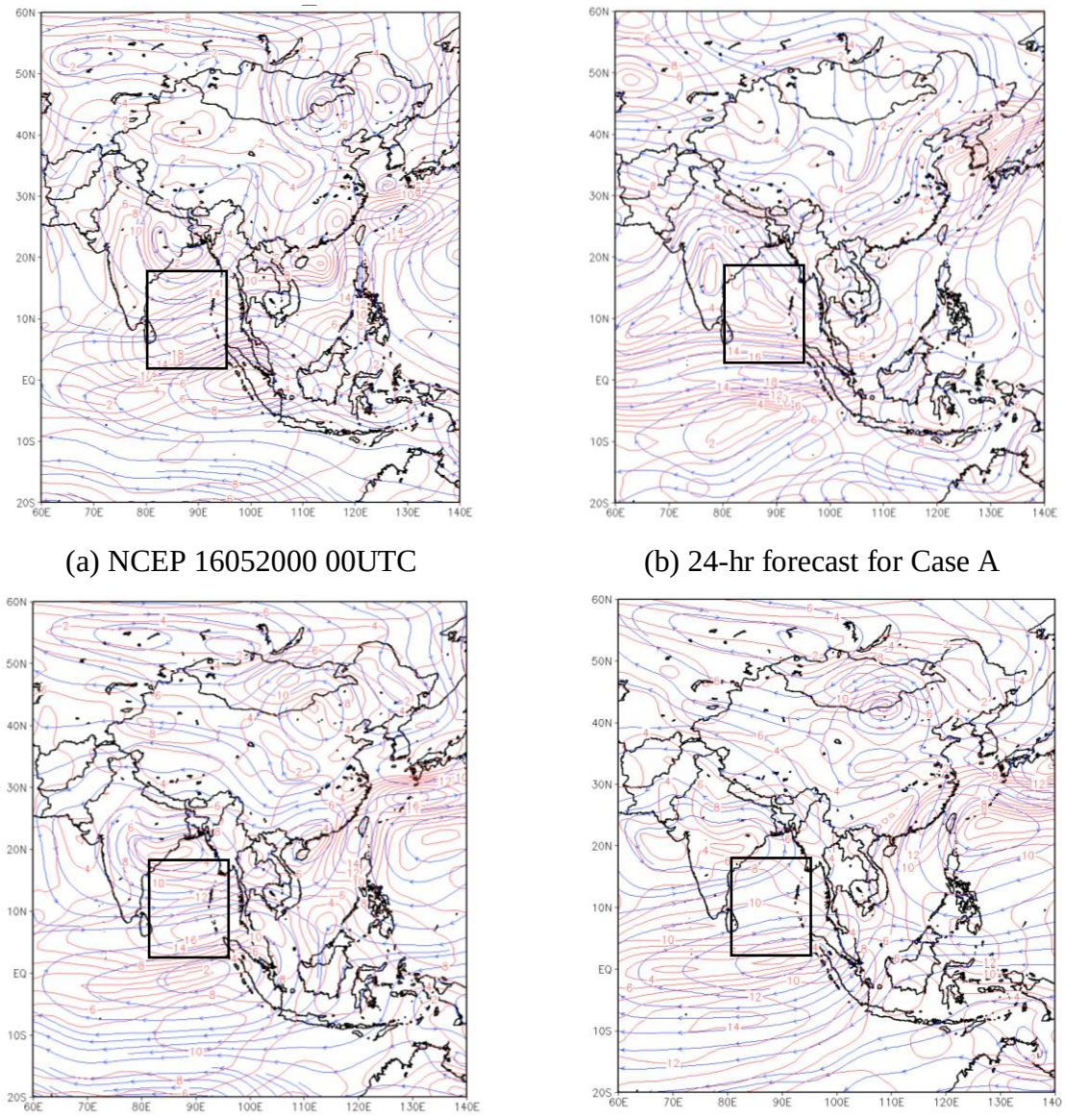

(a) NCEP 16052000 00UTC

(b) 24-hr forecast for Case A

(c) NCEP 17052000 00UTC

(d) 48-hr forecast for Case A

Figure 4.2 Comparison between observation NCEP data (a), (c), (e), (g) and the forecasts (b), (d), (f), (h) of the active summer monsoon for Case A.

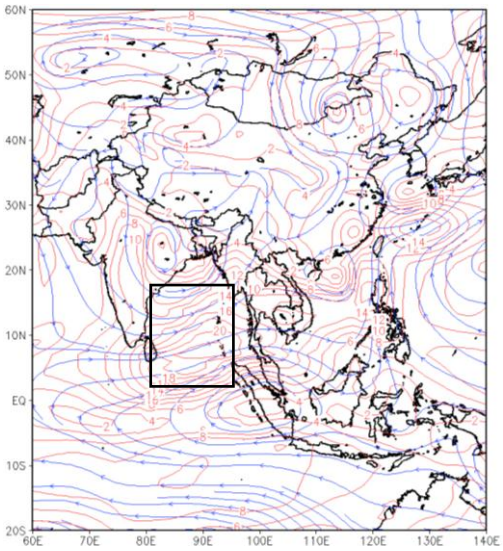

(e) NCEP 18052000 00UTC

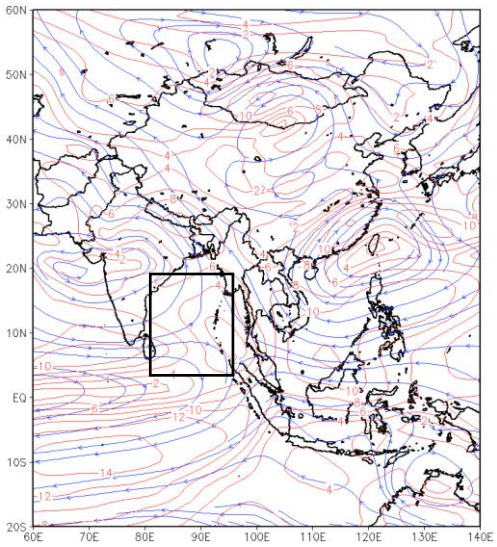

(f) 72-hr forecast for Case A

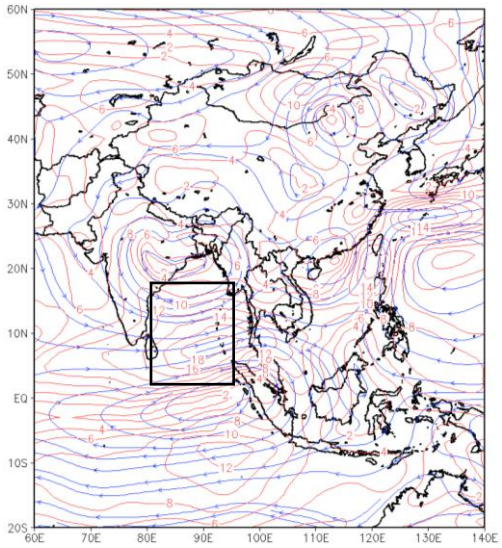

(e) NCEP 19052000 00UTC

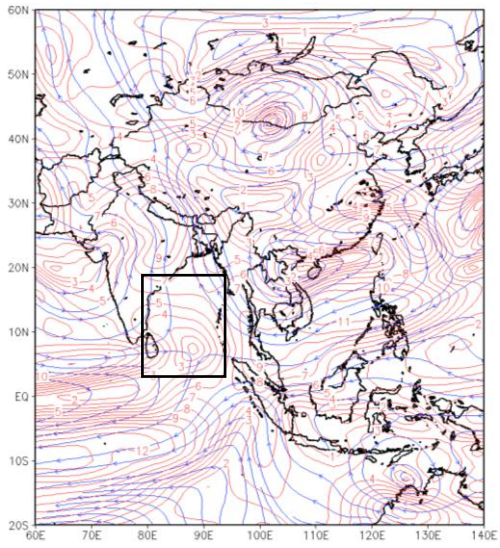

(h) 96-hr forecast for Case A

Figure 4.2 (Cont.)

The results in Figure 4.2 show that acceptable forecast time is about 3 days because wind direction patterns from SILEPE are similar to wind direction from NCEP of Case A in the study domain (black box).

The results from the SILEPE model for Case B are compared with NCEP reanalysis data at the same time in Figure 4.3.

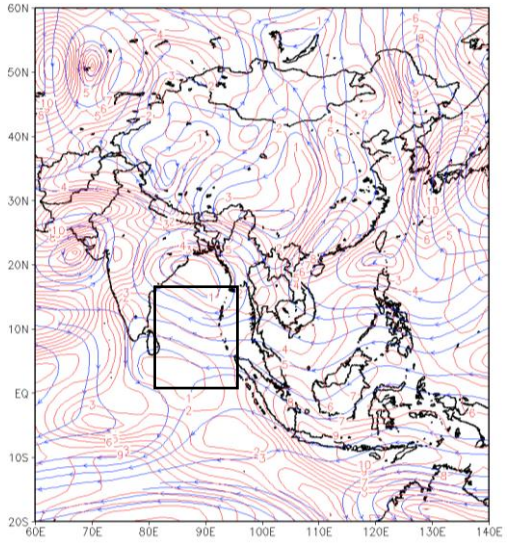

(c) NCEP 02072000 00UTC

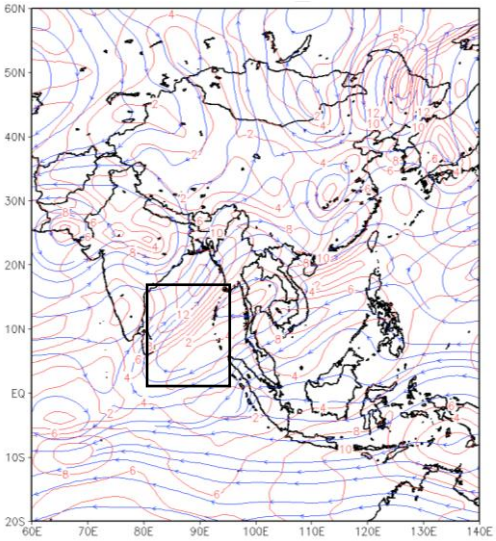

(d) 24-hr forecast for Case B

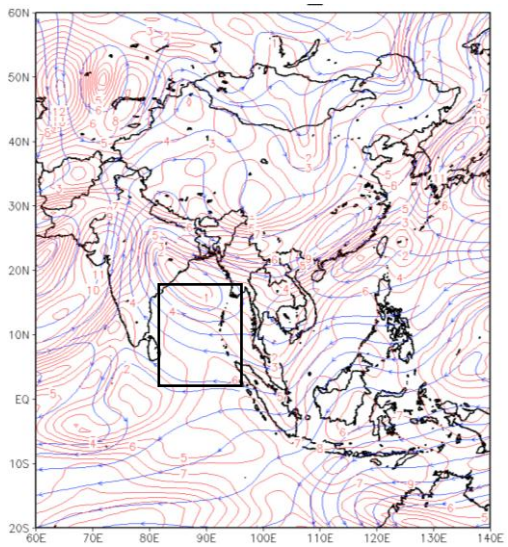

(c) NCEP 03072000 00UTC

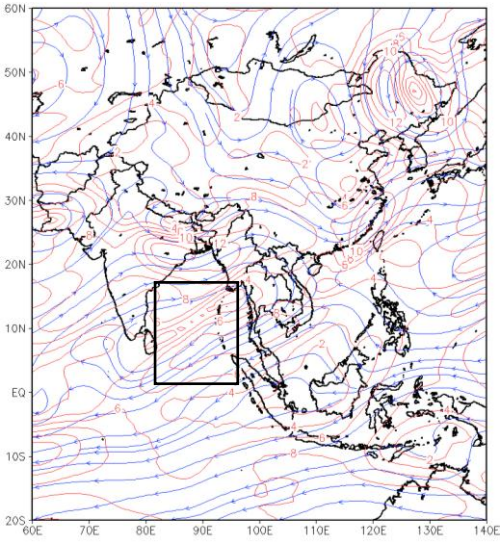

(f) 48-hr forecast for Case B

Figure 4.3 Comparison between observation NCEP data (a), (c), (e), (g) and the forecasts (b), (d), (f), (h) of active summer monsoon for Case B.

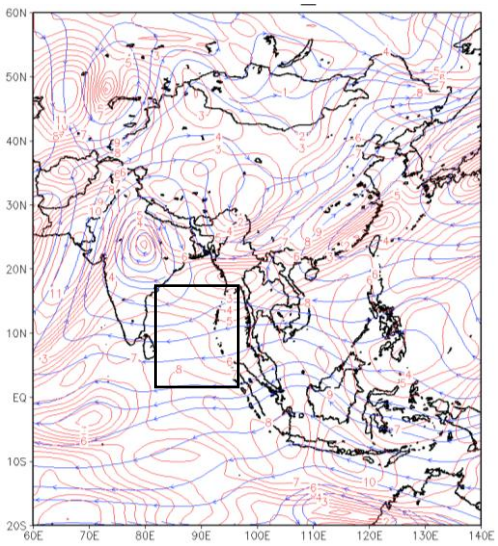

(c) NCEP 04072000 00UTC

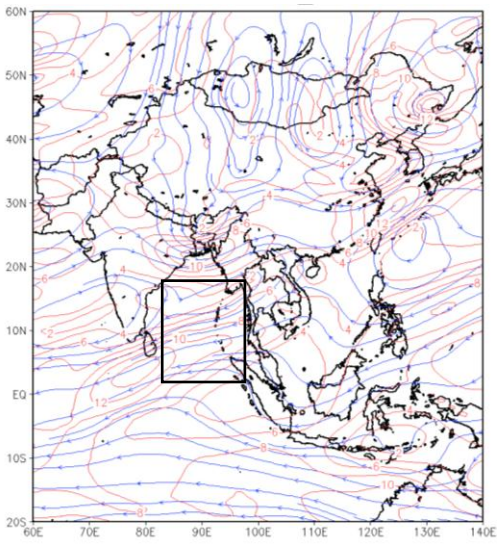

(h) 72-hr forecast for Case B

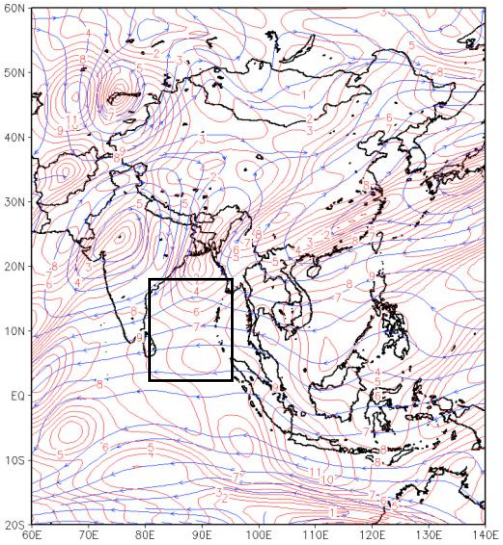

(c) NCEP 05072000 00UTC

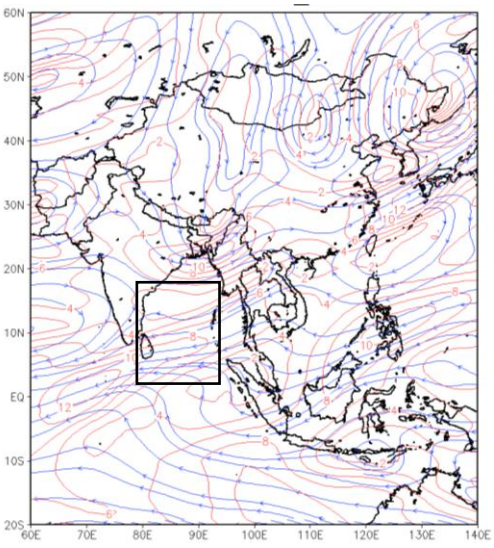

(j) 96-hr forecast for Case B

Figure 4.3 (Cont.)

The results in Figure 4.3 show that acceptable forecast time is about 3 days because wind direction patterns from SILEPE are similar to wind direction from NCEP of Case B in the study domain.

4.2 Control Runs (CTL)

Figure 4.4 shows examples of CTL1 and CTL2. Figures 4.5 (a), (c), (e) and (g) show contour of wind speed (red) and streamline (blue) of IPCC data for active summer monsoon. Figures 4.5 (b), (d), (f) and (h) show contour of wind speed and streamline of A2 scenario at 24, 48, 72 and 96 hours forecasts for active summer monsoon, respectively. While Figures 4.6 (a), (c), (e) and (g) show control run of summer monsoon break of IPCC data. Figures 4.6 (b), (d), (f) and (h) show contour of wind speed and streamline of A2 scenario at 24, 48, and 96 hours forecasts for summer monsoon break, respectively.

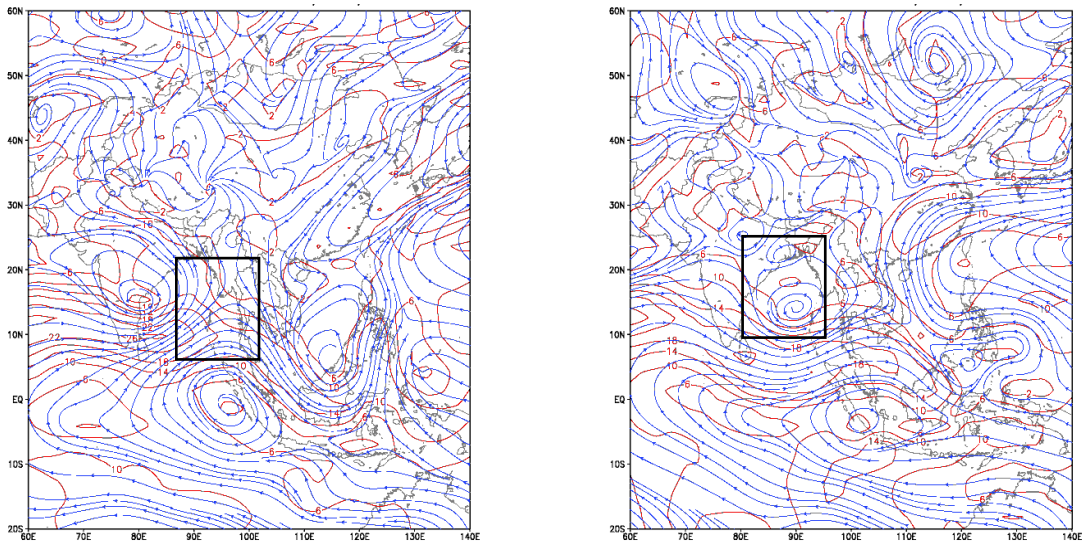

(a) 12 May 2086 for A2- Scenario (b) 22 July 2086 for A2- Scenario

Figure 4.4 Initial condition of (a) active summer monsoon for Case 1 and (b) summer monsoon break for Case 2.

The results in Figure 4.5 show that acceptable forecast time is about 3 days because wind direction patterns from SILEPE are similar to wind direction from IPCC of Case 1 in the study domain.

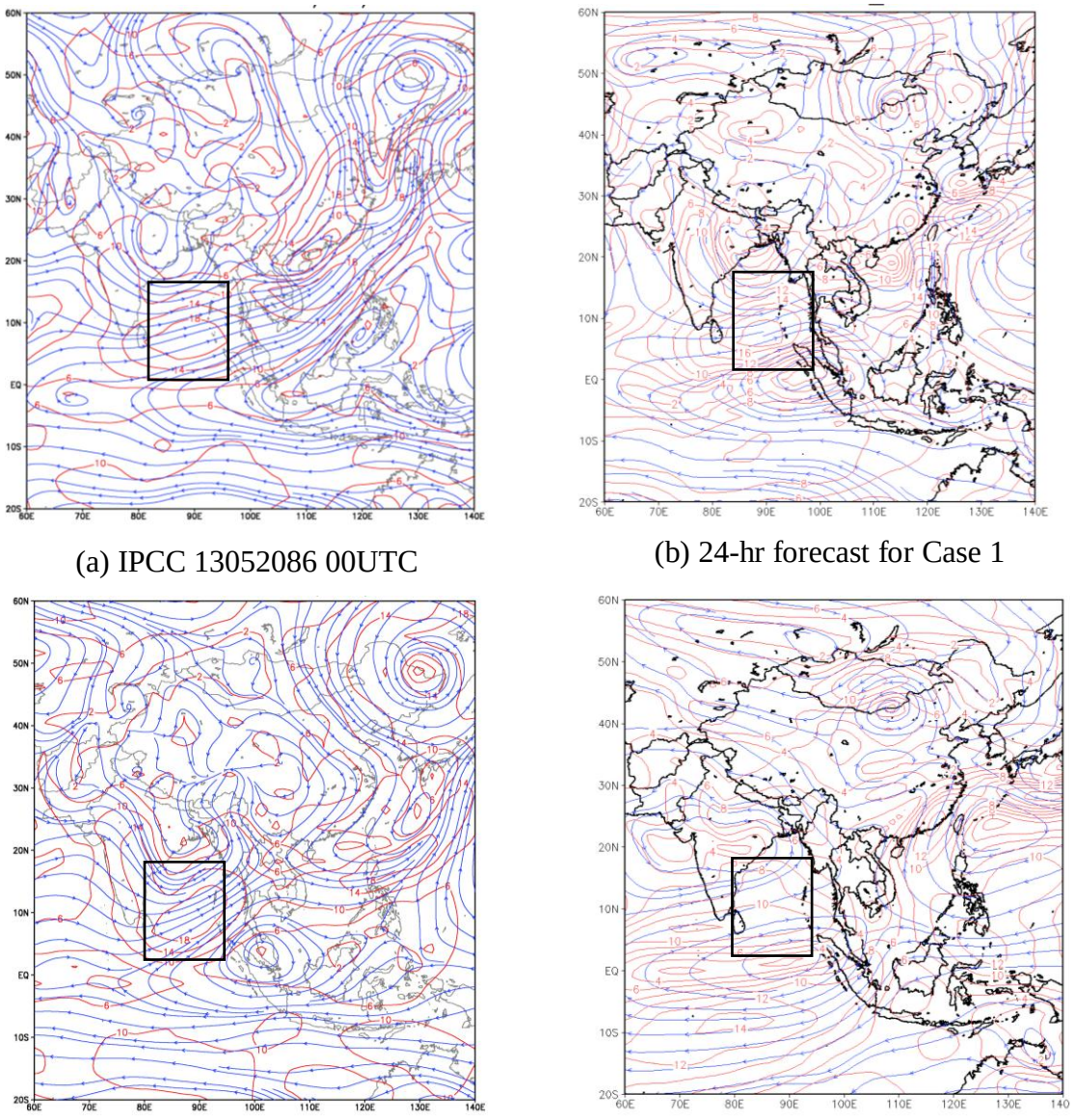

(a) IPCC 13052086 00UTC

(b) 24-hr forecast for Case 1

(c) IPCC 14052086 00UTC

(d) 48-hr forecast for Case 1

Figure 4.5 Comparison between observation IPCC data (a), (c), (e), (g) and the forecasts (b), (d), (f), (h) of active summer monsoon for Case 1.

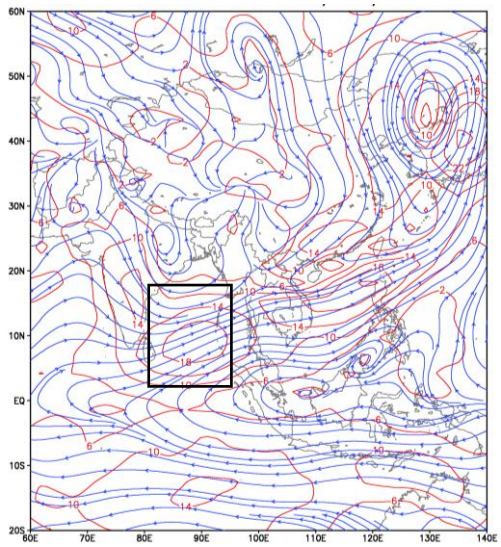

(e) IPCC 15052086 00UTC

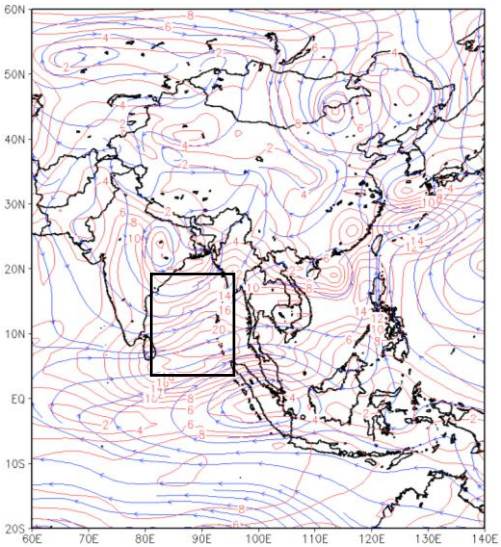

(f) 72-hr forecast for Case 1

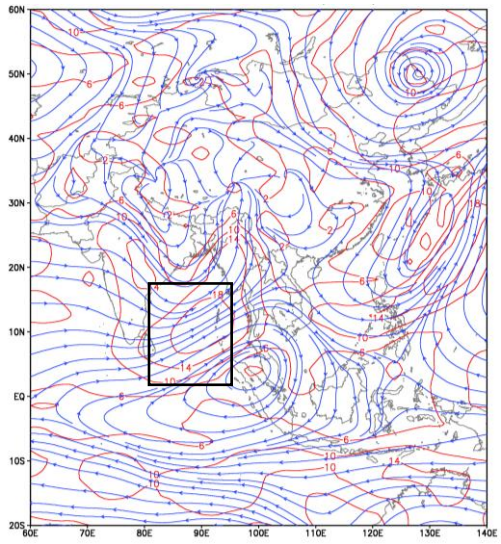

(g) IPCC 16052086 00UTC

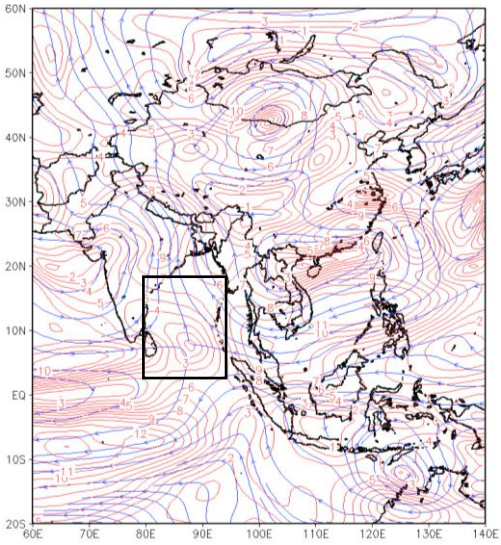

(h) 96-hr forecast for Case 1

Figure 4.5 (Cont.)

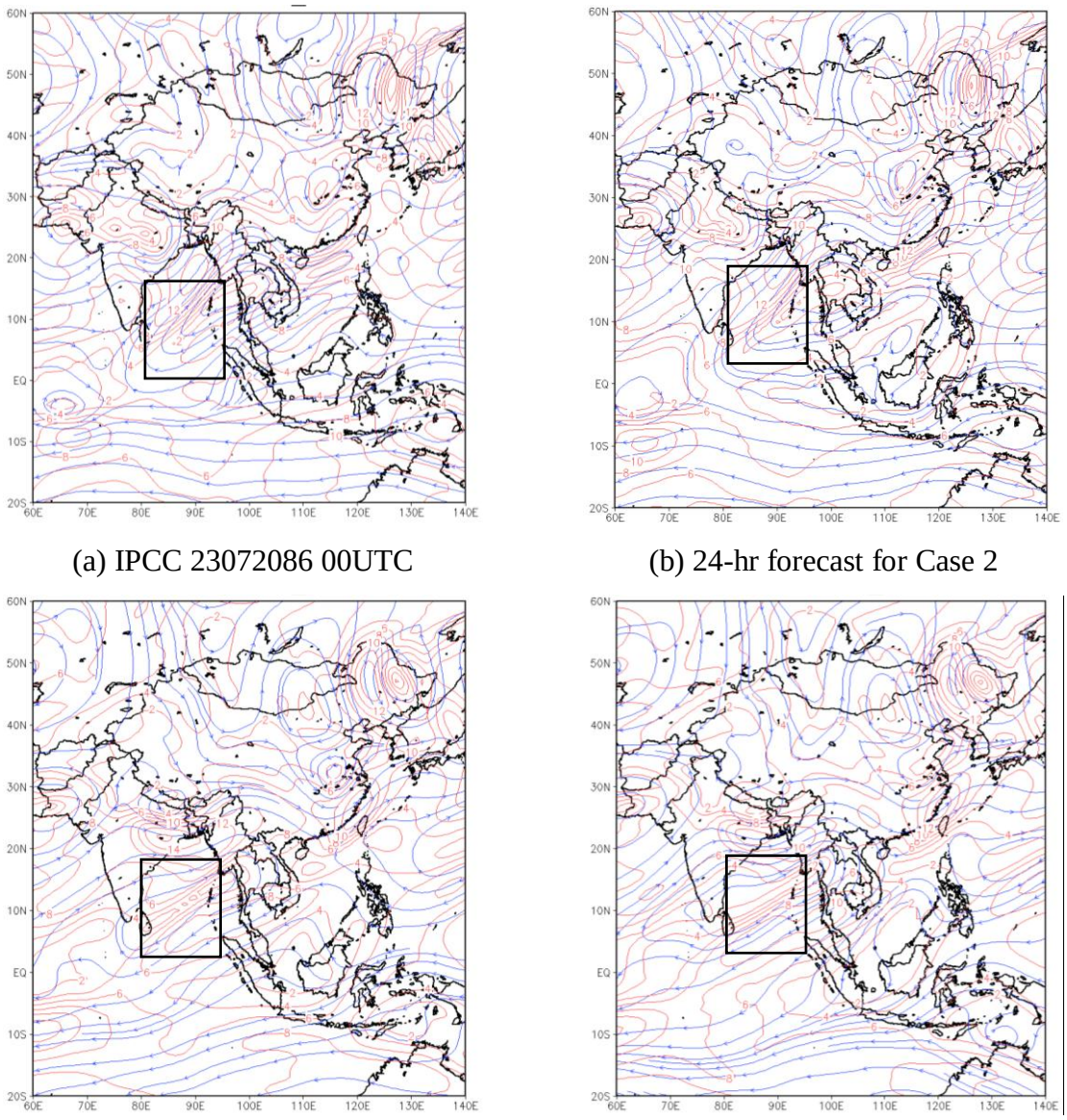

(a) IPCC 23072086 00UTC

(b) 24-hr forecast for Case 2

(c) IPCC 24072086 00UTC

(d) 48-hr forecast for Case 2

Figure 4.6 Comparison between observation IPCC data (a), (c), (e), (g) and the forecasts (b), (d), (f), (h) of active summer monsoon for Case 2.

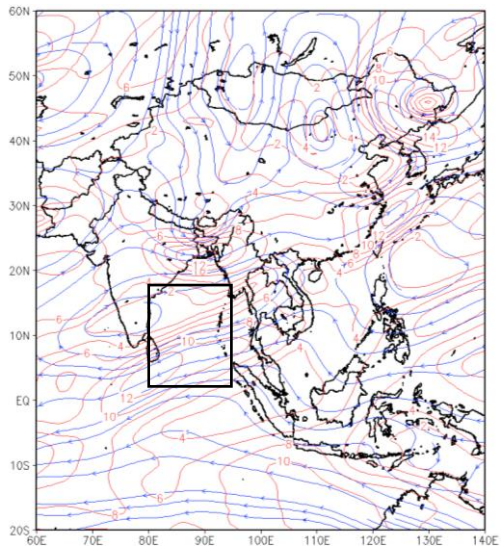

(e) IPCC 25072086 00UTC

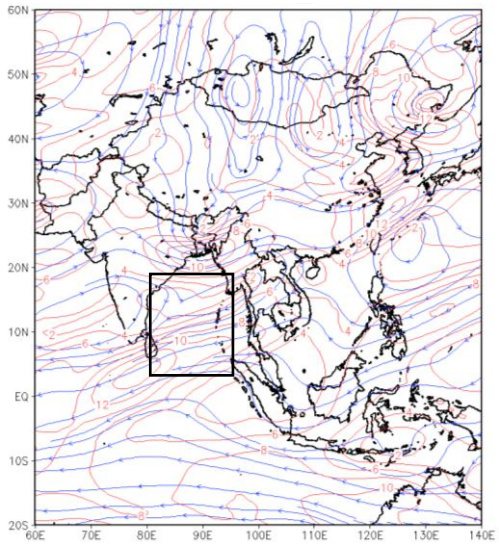

(f) 72-hr forecast for Case 2

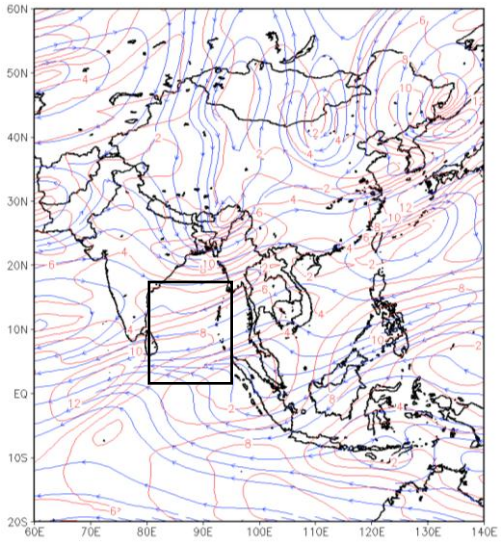

(g) IPCC 26072086 00UTC

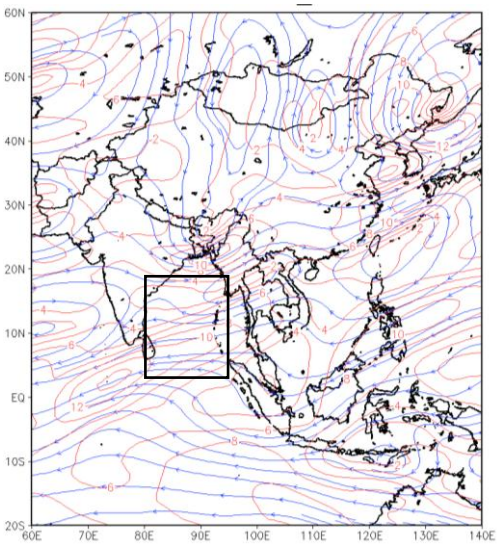

(h) 96-hr forecast for Case 2

Figure 4.6 (Cont.)

The results in Figure 4.6 show that acceptable forecast time is about 4 days because wind direction patterns from SILEPE are similar to wind direction from IPCC of Case 2 in the study domain. The SILEPE cannot be used for long-time run because the model is influenced by the boundary condition. The boundary condition in SILEPE model is not updated every time step and results in poor long-range forecast. However, 3-day forecast is enough for the purpose of this study.

4.3 Singular Vector Ensemble Forecasting

The initial perturbation is generated by the singular vector according to the flow chart in Figure 3.6. Singular vector is performed for only zonal wind component (u) and meridinal wind component (v). The reason for this is to simplify the calculation procedure in finding the singular vector. The geopotential height is obtained from the balance equation (Eq. 2.54). The 50 ensemble members are generated from linearize version of the SILEPE model with various perturbations. To illustrate all ensemble members distribution, wind speed can be express as a spaghetti plot as shown in Figure 4.7 and Figure 4.8. In these figures, green line represents CTL, pink line represents the scenarios from BCCR-BCM2.0, blue line represents plus perturbation (+PRT) and red line represents minus perturbation (-PRT). In this research, final perturbations are only slight perturbed for each experiment. Therefore, scales factor is multiplied to final perturbations. The scale factor of 1.4 is enough to create initial perturbation data.

4.3.1 Active Summer Monsoon

In Figure 4.7, spaghetti plot of wind speed of 18 m/s shows spread of ensemble perturbation. Green color represents CTL, pink color means A2 or COMMIT scenario, blue color is plus perturbation (+PRT), and red color shows minus perturbation (-PRT).

Figure 4.7 demonstrates that ensemble members for both +PRT and -PRT are better ensembles at 24-hr and 48-hr than 72-hr and 96-hr due to the limitation of SILEPE on long-range forecast. The wind speed contour of ensemble members cover control run and A2 in 24-hr forecast. In 48-hr forecast, the ensemble members spread more than in 24-hr forecast but cover control run and A2 only in some regions. The ensemble members cover the region that control run is close to A2. In 96-hr forecast, the ensemble members spreading decrease when compare with the other forecast times.

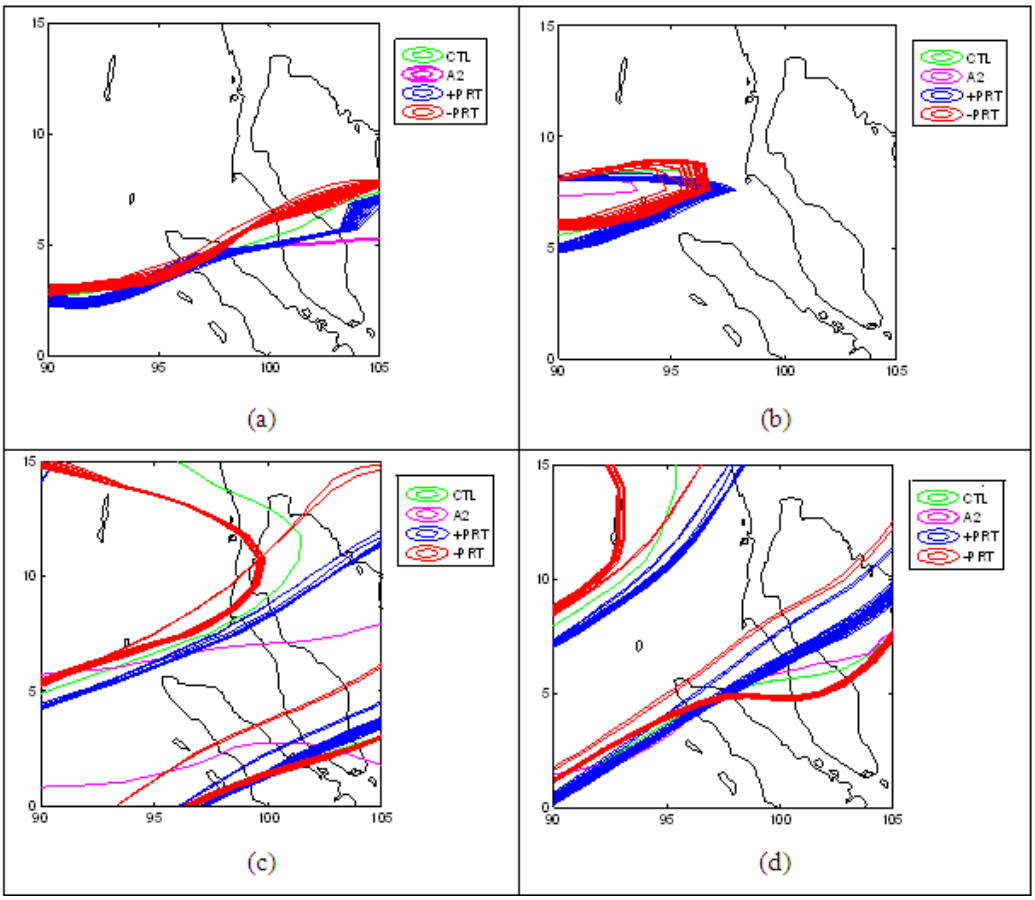

Figure 4.7 Spaghetti plots of 18 m/s wind speed, (a) 24-hr, (b) 48-hr, (c) 72-hr, and (d) 96-hr of Case 1.

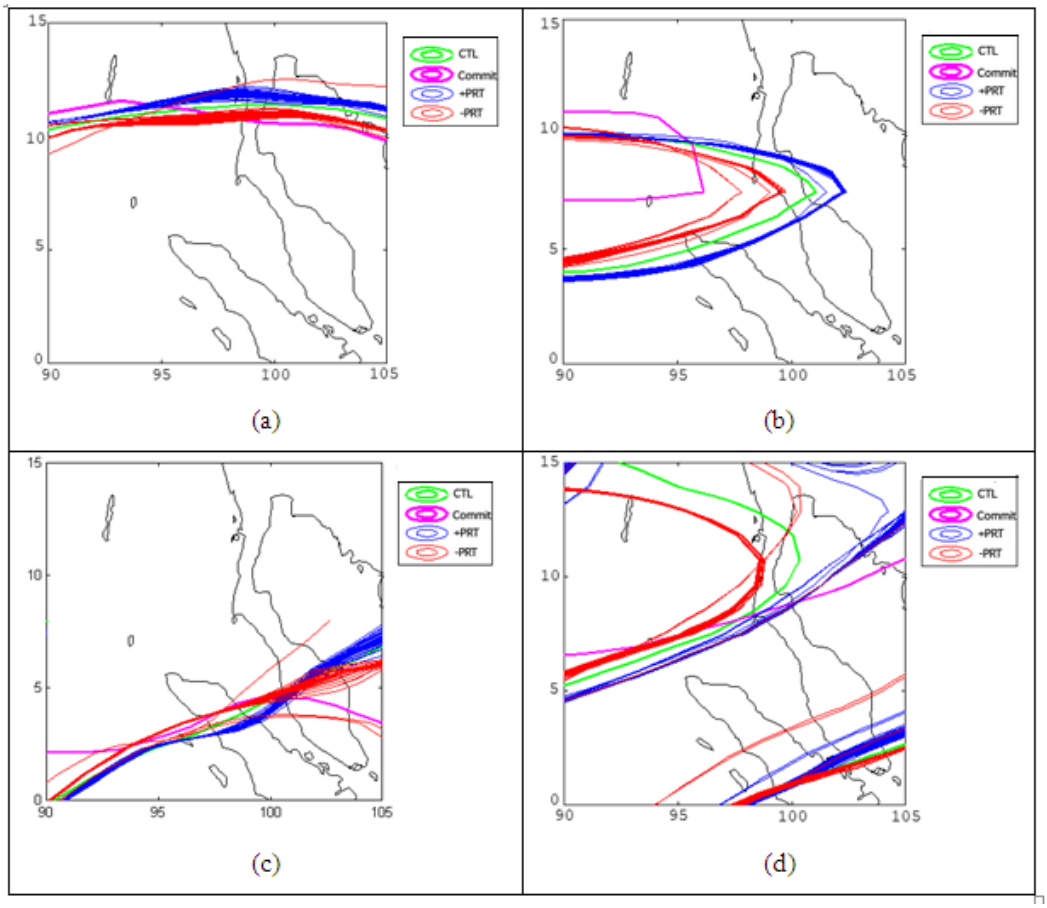

Figure 4.8 Spaghetti plots of 18 m/s wind speed, (a) 24-hr, (b) 48-hr, (c) 72-hr, and (d) 96-hr of Case 3.

In Figure 4.8 spaghetti plot of COMMIT on active monsoon event shows that +PRT and –PRT are good ensembles in 24-hr forecast, because the spreading cover CTL and cover COMMIT in some regions and close to COMMIT. In 48-hr forecast, +PRT and –PRT cover CTL but do not cover COMMIT over some regions. However, most of the forecast patterns are similar to COMMIT, except for +PRT at 72-hr forecast. Also, at 96-hr forecast, both +PRT and –PRT cover CTL and COMMIT over some regions. Both of 2 scenarios indicate more spread of wind speed of A2 than COMMIT.

4.3.1.1 Directional Mean and Circular Variance

Wind directions in Figure 4.9 are examples to show wind directions of Case 1 which are southwest winds. Figure 4.9 shows that almost all of ensemble wind directions follow A2 scenario from BCM-BCCR.2.0 wind direction with only slight difference.

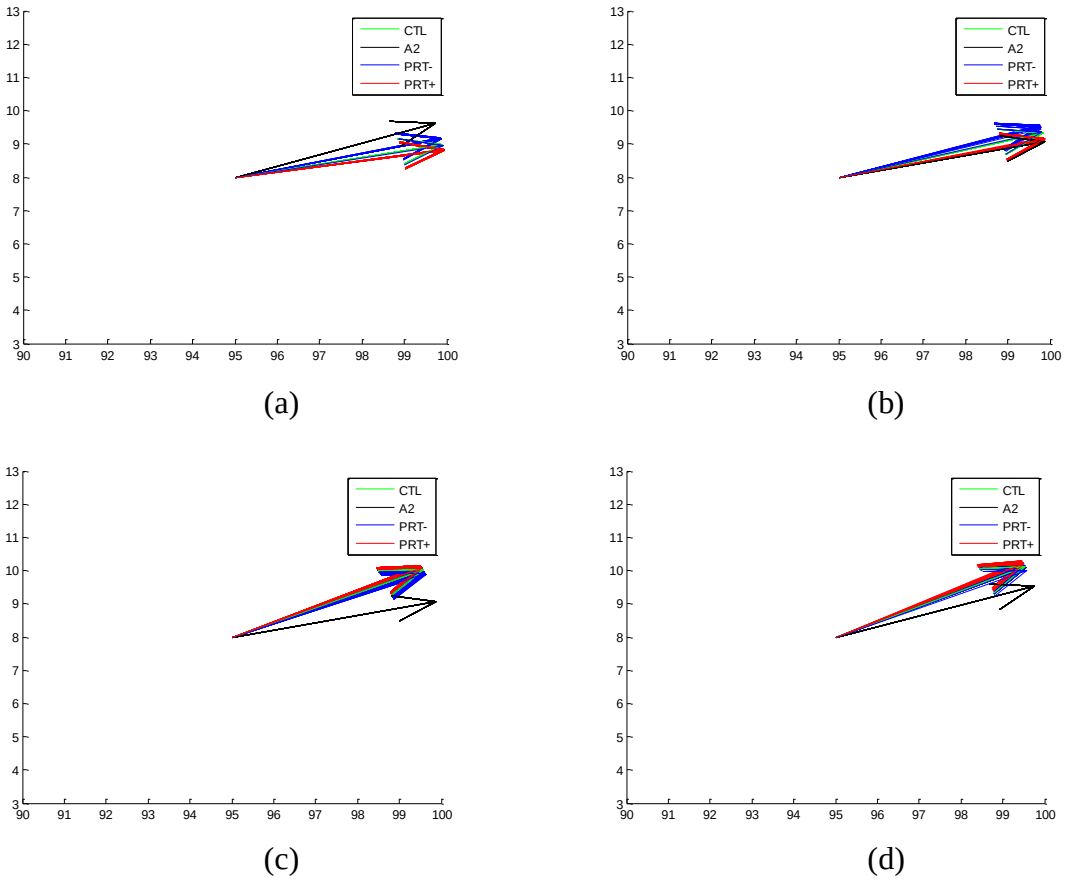

Figure 4.9 Directional mean, (a) 24-hr, (b) 48-hr, (c) 72-hr, and (d) 96-hr for Case 1.

Table 4.1 The value of the directional mean (degree) and the circular variance at 24-hr forecast for Case 1.

Ensemble Member	1	2	3	4	CTL	A2
Direction Mean	9.75	13.22	9.67	13.25	10.45	13.54
Circular Variance	0.00356	0.01687	0.00366	0.01569	0.00180	0.03472

The value of the directional mean and circular variance at 24-hr forecast are shown in Table 4.1 for ensemble members 1 to 4, control run and A2. The results show that the circular variance for each member is close to zero which means all vectors have similar direction.

Figure 4.10 shows that almost all of ensemble wind directions follow COMMIT scenario from BCM-BCCR.2.0 wind direction with slight difference.

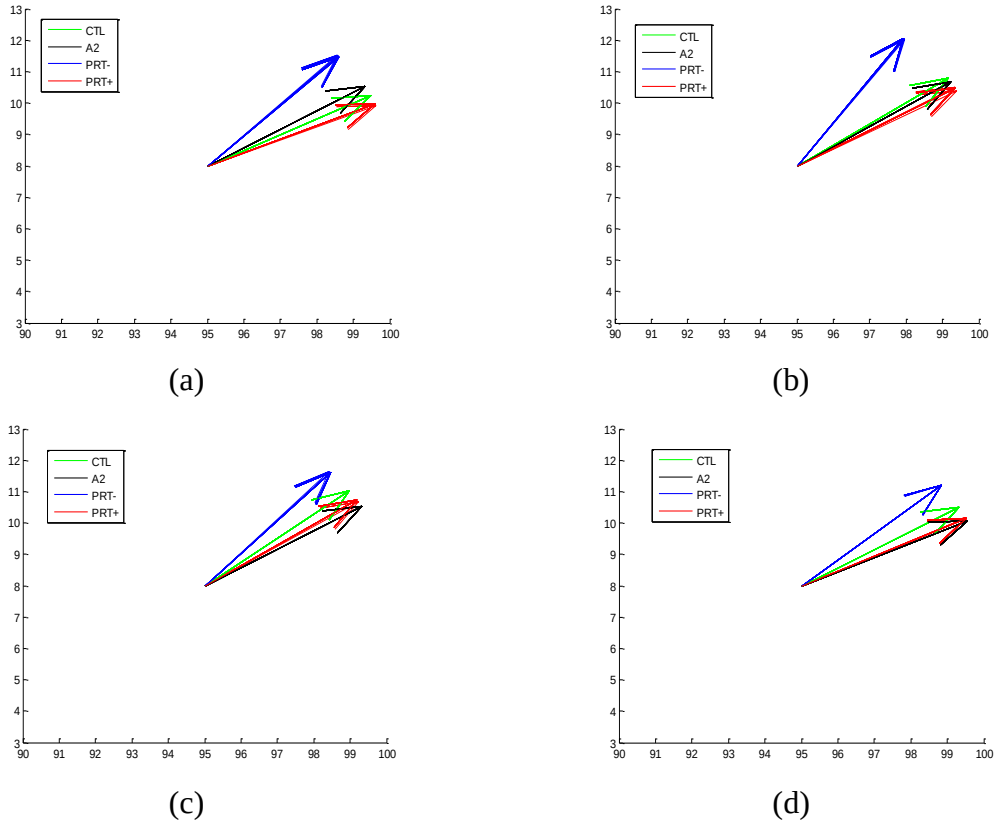

Figure 4.10 Directional mean, (a) 24-hr, (b) 48-hr, (c) 72-hr, and (d) 96-hr for Case 3.

Table 4.2 The value of the directional mean and the circular variance at 24-hr forecast for Case 3.

Ensemble Member	1	2	3	4	CTL	A2
Direction Mean	53.79	29.65421	54.00	28.45	54.17	29.67
Circular Variance	0.00253	0.04657	0.00445	0.02465	0.00237	0.05626

The value of the directional mean and circular variance at 24-hr forecast are shown in Table 4.2 for some ensemble members, control run and COMMIT. The results show that all vectors have similar direction.

4.3.1.2 Ensemble Forecast Probability

From Section 4.3.1, there appears to be a significant uncertainty in the initial condition and forecast of the 18 m/s wind speed in most of the 24-hr and 48-hr forecasts which are considered as "good ensemble". After that, the ensemble members are smoothed and not cover A2 which are considered as "bad ensemble". The smoothing could occur from the finite difference schemes in SILEPE model. The relationship of ensemble forecasts to A2 and COMMIT scenario over Southeast Asia can be expressed in terms of ensemble forecast probability. The ensemble forecast probability is calculated as the fraction of the number of ensemble members that have the same error range with all ensemble members. It can be calculated by Eq. (3.50).

Ensemble forecast probability is a method to show probability of ensemble member that satisfies the event E for each grid point. To start, find the error value between A2 or COMMIT scenarios with each ensemble member (including control run). The 51 members are counted to find probability. Ensemble forecast probability is considered in 2 categories, error not over 5% and error not over 7.5%. Wind speed and direction are selected for finding ensemble forecast probability. In Table 4.3, the grid point $9^{\circ}N,\ 91^{\circ}E$ has probability 78% for $\pm 5\%$ error which means that 39 out of 50 ensemble members are in the range of $\pm 5\%$ error. While probability 100% has all ensemble members in the range of $\pm 7.5\%$ error.

Table 4.3 Example of the number of ensemble member that corresponds to the event at each grid point in Case 1 for 96-hr forecast.

Grid Point	Error Range (E)	n(E)	n(T)	P(E) (%)
lat: $9^{\circ} N$	$\pm 5\%$	20	50	40
lon: $92^{\circ} E$	$\pm 7.5\%$	27	50	54
lat: $9^{\circ} N$	$\pm 5\%$	39	50	78
lon: $91^{\circ} E$	$\pm 7.5\%$	50	50	100

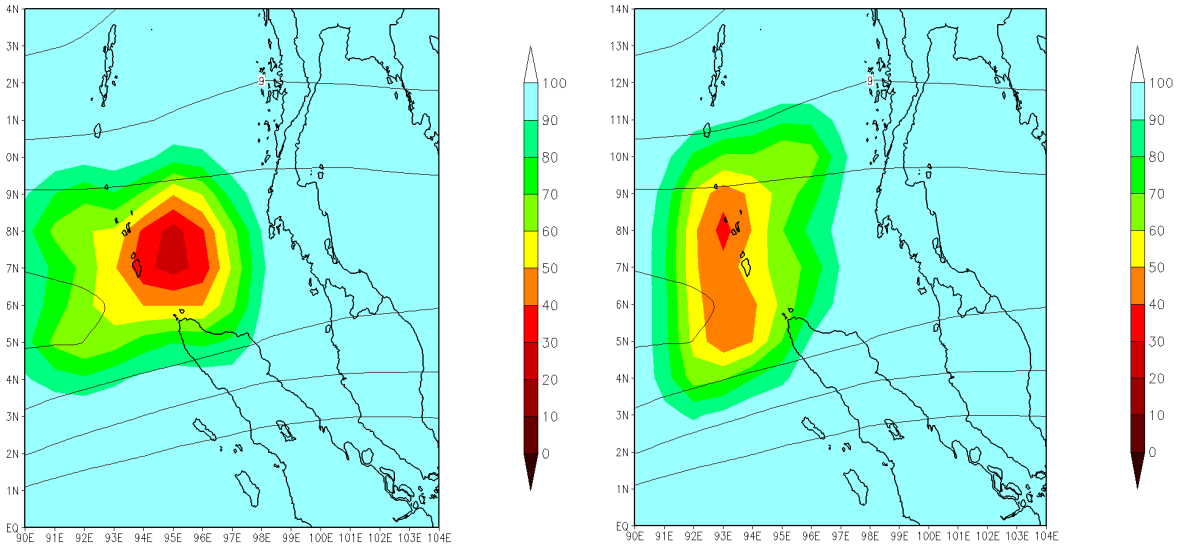

(a) (b)

Figure 4.11 Ensemble forecast probability of wind direction for (a) error range $\pm 5\%$ (b) error range $\pm 7.5\%$ for Case 1 at 96-hr forecast.

Figure 4.11 shows ensemble forecast probability of wind direction for 96-hr forecast of Case 1 for (a) error range $\pm 5\%$ and (b) error range $\pm 7.5\%$. Over Indochina peninsular the probability is greater than 80%. Thus, these are consistency of ensemble forecast which implies good reliability of BCMCRR_BCM2 simulations.

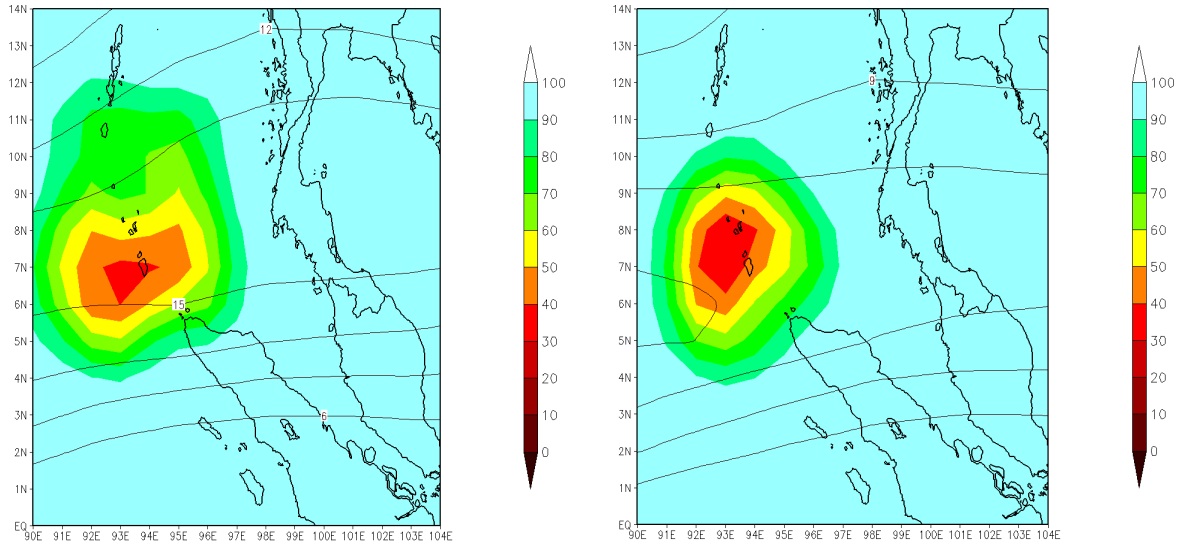

(a) (b)

Figure 4.12 Ensemble forecast probability of wind speed for (a) Error range ± 5% (b) Error range ± 7.5% for Case 1 at 96-hr forecast.

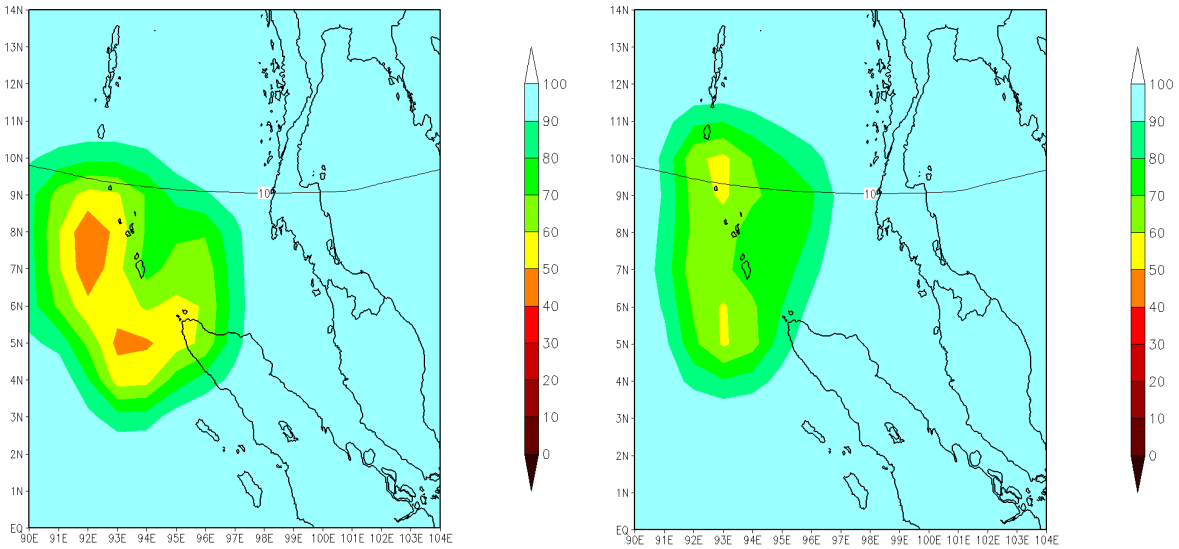

(a)

(b)

Figure 4.13 Ensemble forecast probability of wind direction for (a) Error range ± 5% (b) Error range ± 7.5% for Case 3 at 96-hr forecast.

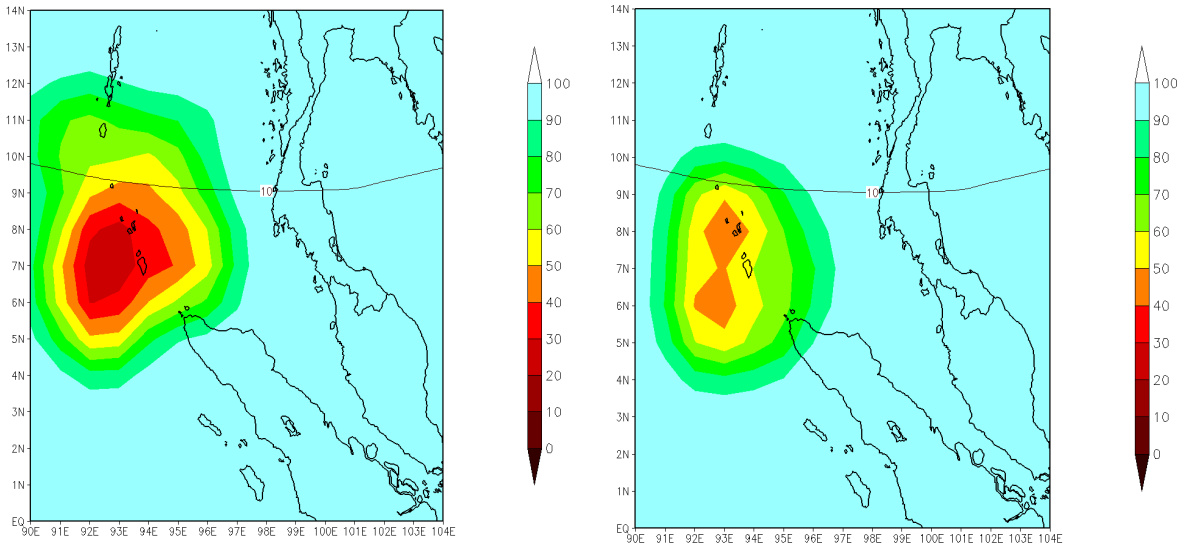

(a) (b)

Figure 4.14 Ensemble forecast probability of wind speed for (a) Error range ± 5% (b) Error range ± 7.5% for Case 3 at 96-hr forecast.

Figures 4.12 shows of ensemble forecast probability of wind speed for 96-hr forecast of Case 1. The probabilities for (a) error range ± 5% and (b) error range ± 7.5% also demonstrate good reliability of wind speed from BCCR_BCM_2.0 simulation.

Ensemble forecast probabilities for Case 3 also show good consistency of BCCR_BCM2.0 in future climate simulation as shown in Figure 4.13 for wind direction and Figure 4.14 for wind speed.

4.3.1.3 Relative Skill Score (RSS)

From Eq. (3.47), for A2 (Case 1)

$$E_{CONTROL} = E_{A2}$$

and

$$E_{ENSEMBLE} = E_{ENSEMBLE\ A2} \text{ (for mean ensemble of A2).}$$

Similarly, for COMMIT (Case 3)

$$E_{CONTROL} = E_{COMMIT}$$

and

$$E_{ENSEMBLE} = E_{ENSEMBLE\ COMMIT} \text{ (for mean ensemble of COMMIT).}$$

Figure 4.15a shows RSS of wind speed for A2 and COMMIT for Cases 1 and 3, respectively. The score for A2 is better than COMMIT. However, in Figure 4.15b, the scores for wind direction for A2 and COMMIT for Cases 1 and 3 are almost the same.

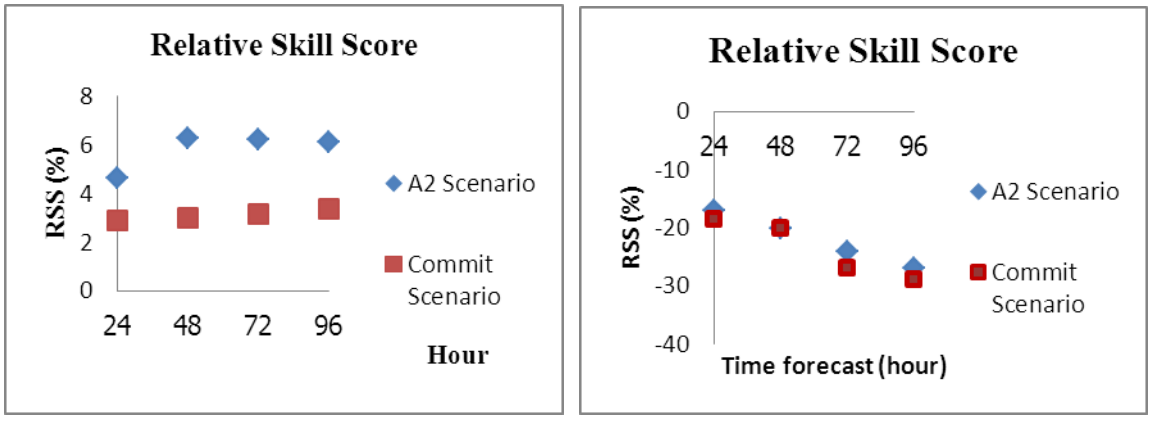

(a) (b)

Figure 4.15 Relative skill score (RSS) for (a) wind speed and (b) wind direction for Case 1 and Case 3.

4.3.2 Summer Monsoon Break

In Figures 4.16 and 4.17, spaghetti plots of wind speed 10 m/s for 24-hr and 48-hr forecasts show spread of ensemble perturbation. The results for summer monsoon break, Case 2 and Case 4 are shown in Figures 4.16 and 4.17, respectively. Results for Case 2 show positive and negative perturbations cover CTL but not cover A2 over some areas at 24-hr and 48-hr forecasts. The 96-hr forecast is a bad ensemble. Figure 4.16 shows that results are good ensembles.

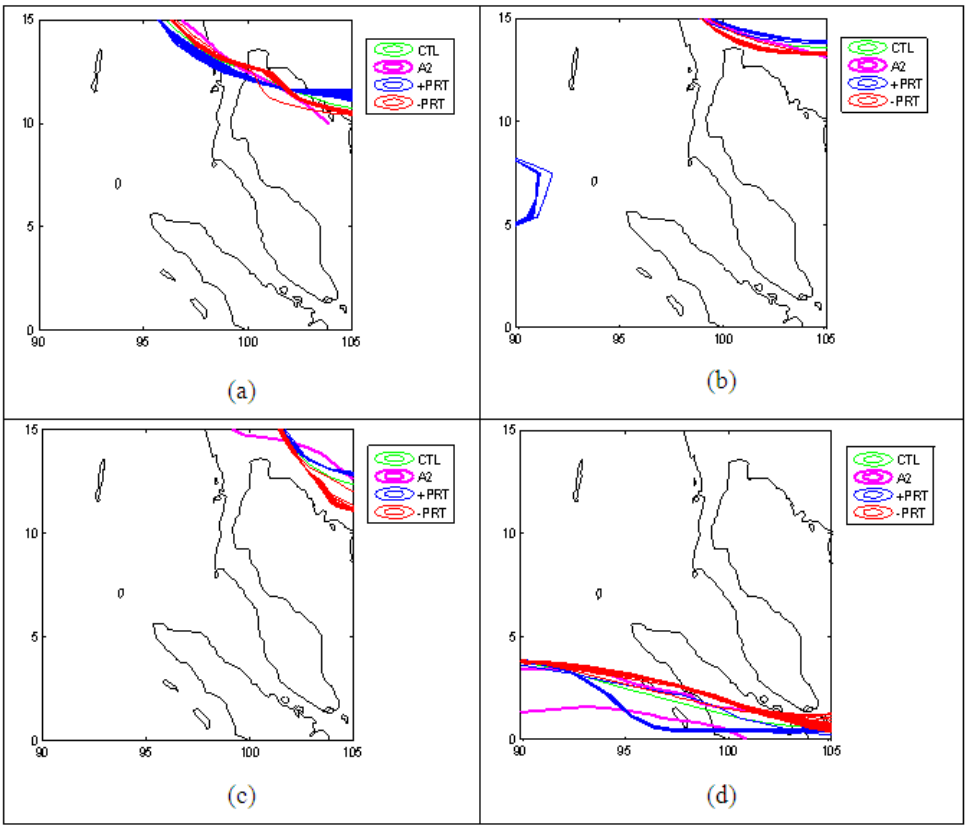

Figure 4.16 Spaghetti plots of wind speed 10 m/s for (a) 24-hr, (b) 48-hr, (c) 72-hr, and (d) 96-hr forecasts of a monsoon break for Case 2.

Results for Case 4 in Figure 4.17 show positive and negative perturbations cover CTL but not cover COMMIT over some areas at 24-hr, 48-hr and 72-hr forecasts. The 96-hr forecast

is a bad ensemble. Figure 4.17 shows that most results are good ensembles except 96-hr forecast.

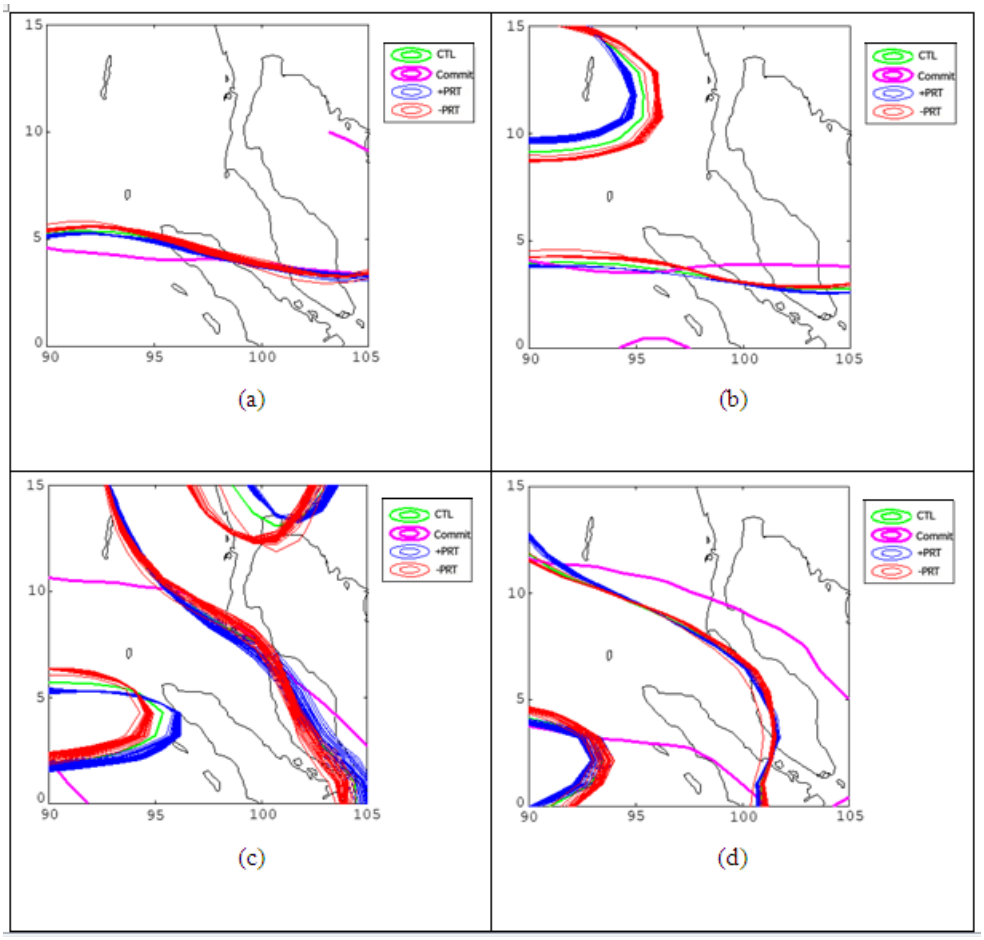

Figure 4.17 Spaghetti plots of wind speed 10 m/s, (a) 24-hr, (b) 48-hr, (c) 72-hr, and (d) 96-hr forecasts for Case 4.

4.3.2.1 Directional Mean and Circular Variance

Wind directions in Figure 4.18 are examples to show wind directions of Case 2 which are westerly winds for 24-forecast and northwesterly for 72-forecast. Figure 4.18 shows that almost all of ensemble wind directions for Case 2 follow A2 scenario from BCM-BCCR.2.0 wind direction with slight difference.

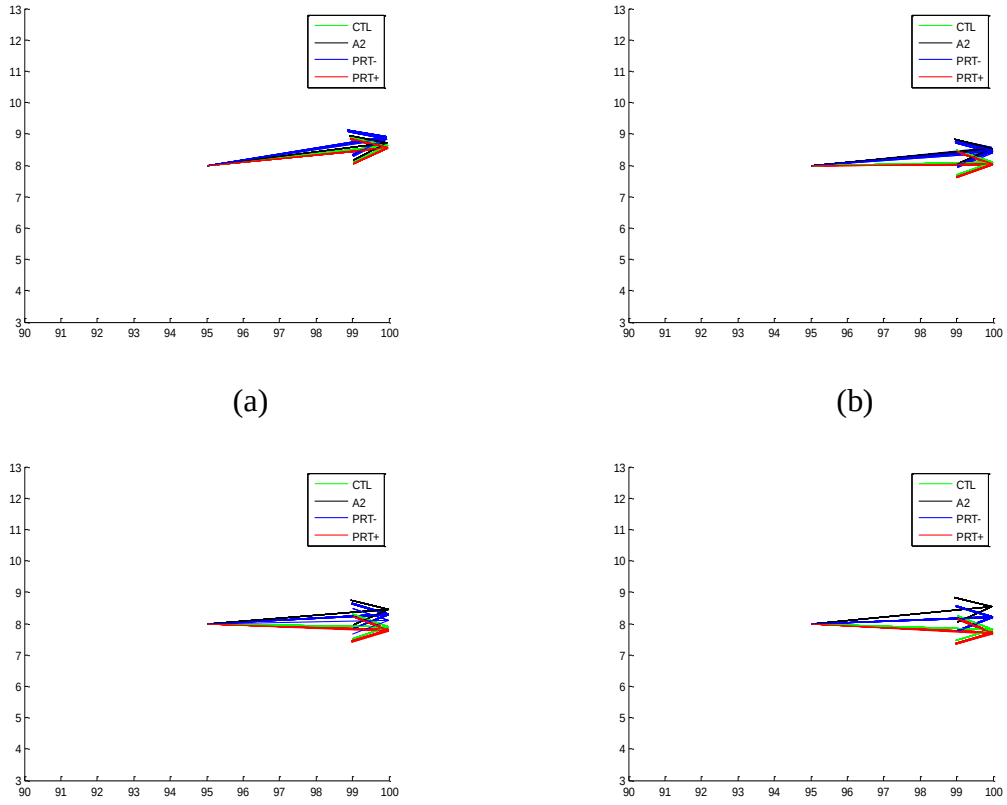

Figure 4.18 Directional mean, (a) 24-hr, (b) 48-hr, (c) 72-hr, and (d) 96-hr for Case 2.

Table 4.4 The value of the directional mean (degree) and the circular variance at 24-hr forecast for Case 2.

Ensemble Member	1	2	3	4	CTL	A2
Direction Mean	6.75	10.28	6.59	10.24	7.16	8.16
Circular Variance	0.00023	0.01725	0.00211	0.01235	0.00174	0.0245

The values of the directional mean and circular variance are shown in Table 4.4 for some ensemble members, control run and A2. The results show that the circular variance for each member is close to zero which means all vectors have similar direction. Similarly, wind direction results from COMMIT (Case 4) also have similar directions as A2.

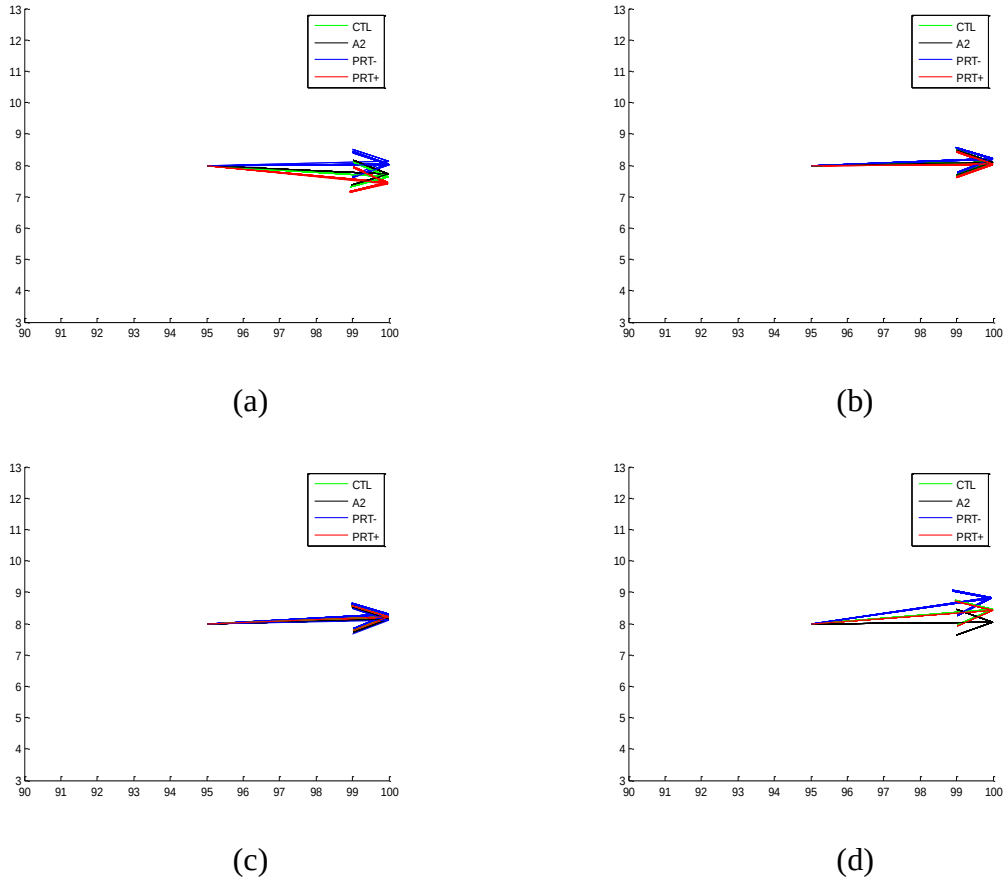

Figure 4.19 Directional mean, (a) 24-hr, (b) 48-hr, (c) 72-hr, and (d) 96-hr for Case 4.

Table 4.5 The value of the directional mean (degree) and the circular variance at 24-hr forecast for Case 4.

Ensemble Member	1	2	3	4	CTL	A2
Direction Mean	-6.441	0.384	-6.378	1.469	-4.168	-3.213
Circular Variance	0.00653	0.00657	0.00346	0.03425	0.00457	0.06246

The values of the directional mean and circular variance are shown in Table 4.5 for some ensemble members, control run and COMMIT. The results show that the circular variance for each member is close to zero.

4.3.2.1 Ensemble forecast Probability

The ensemble forecast probability of wind speed and wind direction for Cases 2 and 4 are shown in Figures 4.20- 4.23.

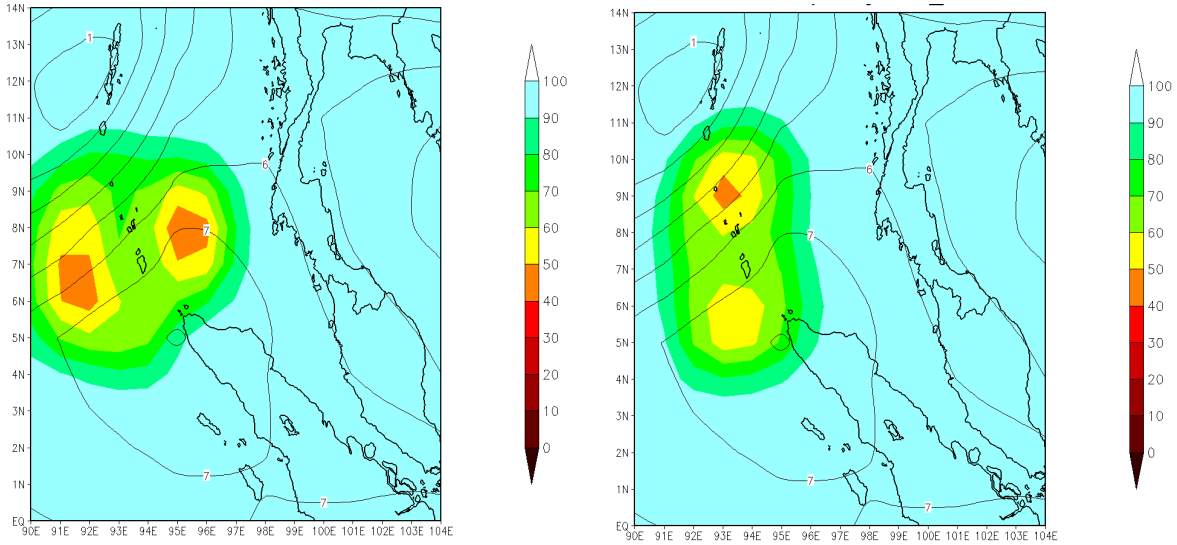

(a) (b)

Figure 4.20 Ensemble forecast probability of wind direction for (a) error range $\pm 5\%$ (b) error range $\pm 7.5\%$ for Case 2 at 96-hr forecast.

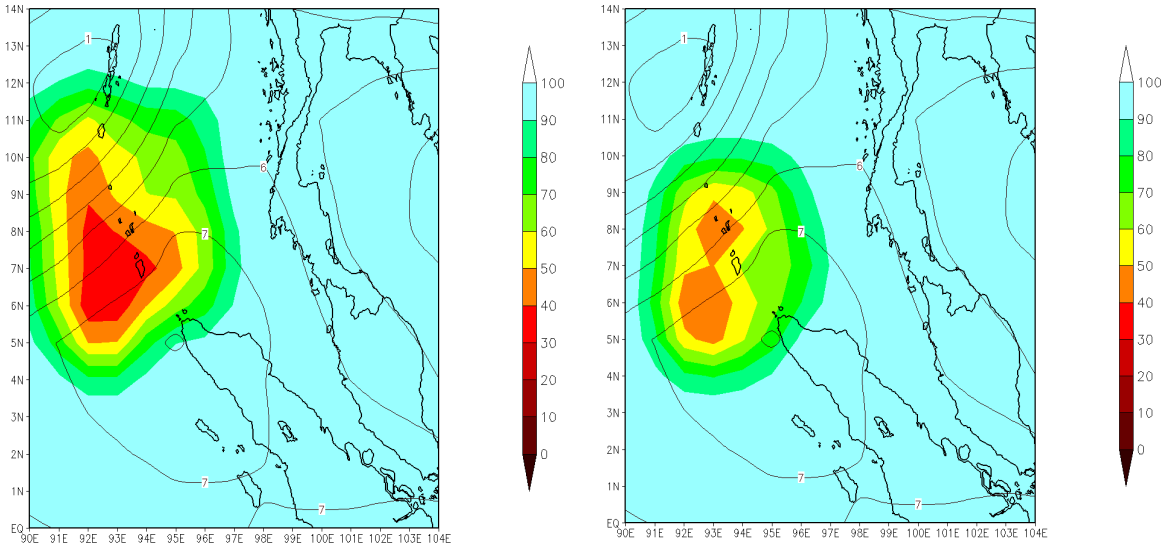

(a) (b)

Figure 4.21 Ensemble forecast probability of wind speed for (a) error range $\pm 5\%$ (b) error range $\pm 7.5\%$ for Case 2 at 96-hr forecast.

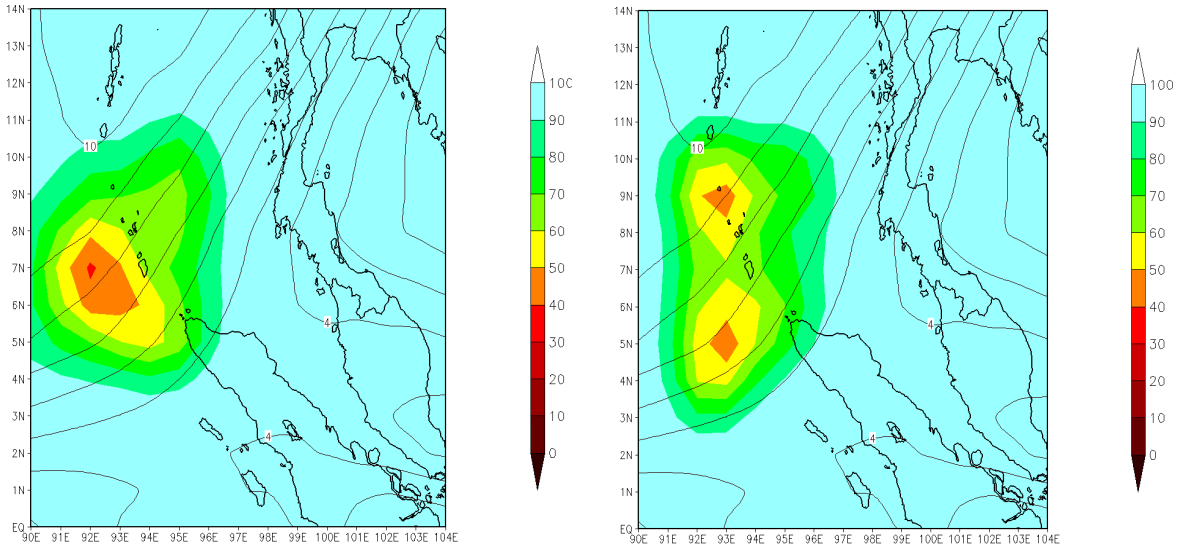

(a) (b)

Figure 4.22 Ensemble forecast probability of wind direction for (a) error range $\pm 5\%$ (b) error range $\pm 7.5\%$ for Case 4 at 96-hr forecast.

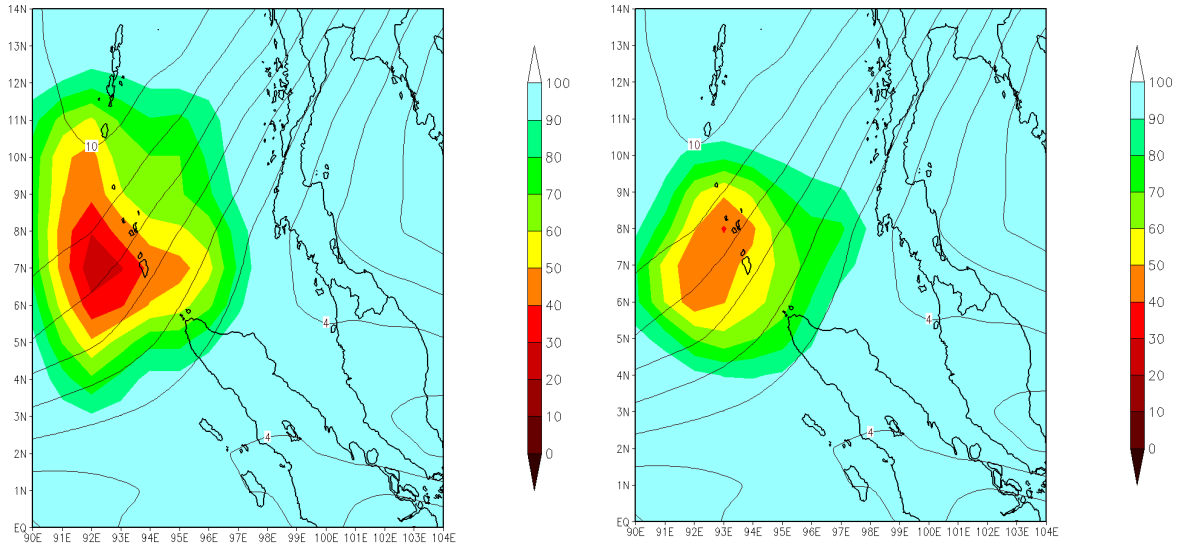

(a) (b)

Figure 4.23 Ensemble forecast probability of wind speed for (a) error range $\pm 5\%$ (b) error range $\pm 7.5\%$ for Case 4 at 96-hr forecast.

Ensemble forecast probabilities for Case 2 and 4 are shown in Figures 4.20 – 4.23. Similar to those of active cases the results show that the ensemble forecasts have small error range. Thus, results from BCCR_BCM2.0 simulation are reliable.

4.3.2.2 Relative Skill Score

From Eq. (3.47), for A2 (Case 2)

$$E_{CONTROL} = E_{A2}$$

and

$$E_{ENSEMBLE} = E_{ENSEMBLE\ A2} \text{ (for mean ensemble ofA2).}$$

Similarly, for COMMIT (Case 4)

$$E_{CONTROL} = E_{COMMIT}$$

and

$$E_{ENSEMBLE} = E_{ENSEMBLE\ COMMIT} \text{ (for mean ensemble of COMMIT).}$$

The RSS for Cases 2 and 4 are shown in Figure 4.24 which are similar to the active cases. The score for speed of A2 is better than COMMIT.

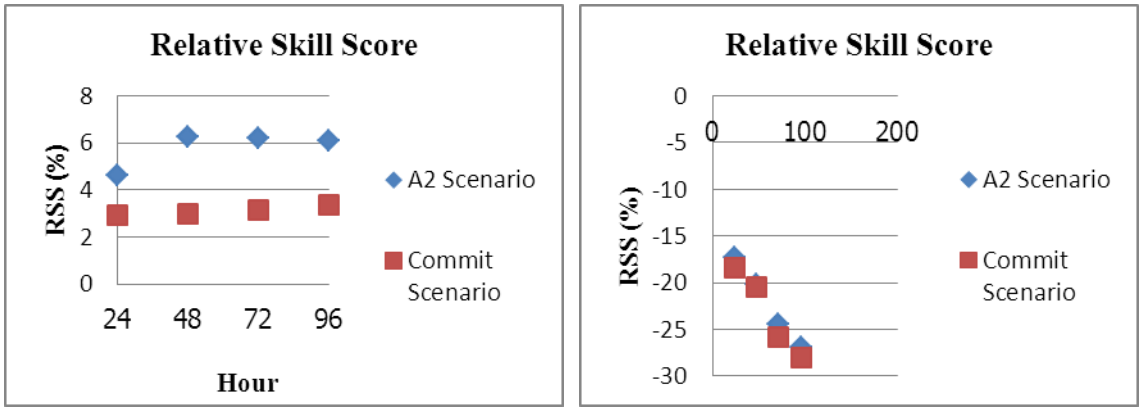

(a) (b)

Figure 4.24 Relative skill score (RSS) for (a) wind speed, and (b) wind direction for Case 2 and Case 4.

4.4 Characteristics of the Monsoon

The results of all experiments show that the BCCR_BCM2.0 simulations are reliable and characteristics of active and break of the summer monsoon can be analyzed as follows.

Active Monsoon

In case of wind direction, the results show that active summer monsoon has strong southwesterly wind over the Bay of Bengal and Indochina Peninsula.

For wind speed, during the active monsoon wind speed is about 18 ms^{-1} over the Bay of Bengal and extends to cover Indochina Peninsula and increases to about 20 ms^{-1} over South China Sea.

Monsoon Break

In case of wind direction, the results show that summer monsoon break has westerly wind over the Bay of Bengal and Indochina Peninsula. The monsoon break periods are associated with a weakened monsoonal circulation.

For wind speed, during the monsoon break wind speed is about 14 ms^{-1} over the Bay of Bengal and Indochina Peninsula.